Toward an understanding of fibrin branching structure

Aaron L. Fogelson* and James P. Keener†
Department of Mathematics and Department of Bioengineering, University of Utah, 155 South 1400 East, Room 233 JWB Salt Lake City, Utah 84112, USA
(Received 27 January 2010; published 24 May 2010)

The blood clotting enzyme thrombin converts fibrinogen molecules into fibrin monomers which polymerize to form a fibrous three-dimensional gel. The concentration of thrombin affects the architecture of the resulting gel, in particular, a higher concentration of thrombin produces a gel with more branch points per unit volume and with shorter fiber segments between branch points. We propose a mechanism by which fibrin branching can occur and show that this mechanism can lead to dependence of the gel's structure (at the time of gelation) on the rate at which monomer is supplied. A higher rate of monomer supply leads to a gel with a higher branch concentration and with shorter fiber segments between branch points. The origin of this dependence is explained.

DOI: 10.1103/PhysRevE.81.051922 PACS number(s): 87.15.A−, 87.15.R−, 87.15.hg

I. INTRODUCTION

The formation of a fibrin protein gel, or fibrin clot, is an important component of the blood clotting process. The structure of the fibrin clot (branch points per unit volume, fiber thickness, pore sizes, etc.) is sensitive to the conditions under which the gel is formed. The viscoelastic mechanical properties of the clot are very sensitive to its structure and the clot's structure also affects the facility with which the fibrinolytic system can degrade the clot [1]. Variations in clot structure have been correlated with bleeding or thrombotic tendencies [2–4].

One of the factors that influences the structure of a fibrin clot is the concentration of the coagulation enzyme thrombin. Thrombin produces fibrin monomer from a precursor molecule, fibrinogen, and so the concentration of thrombin presumably influences the rate of supply of monomer during fibrin polymerization and gelation. A goal of this paper is to gain insight into how the rate at which monomer is supplied can affect the structure of the resulting gel.

Fibrinogen is an elongated trinodular molecule with a central *E* region connected by coiled-coil chains to two *D* regions. Fibrin monomers are produced when thrombin cleaves two short protein fragments from the E region. This uncovers two "*A*" sites each of which can bind to a constitutively exposed complementary "*a*" site in the *D* region of another fibrin(ogen) molecule. This binding process leads to spontaneous polymerization of fibrin monomers into long half-staggered (because of the middle to end binding) double-stranded protofibrils. When sufficiently long, these strands can bind side by side to form thicker fibers in a process known as lateral assembly. Somewhere during the formation of a protofibril and/or during lateral assembly branches form and eventually a three-dimensional fibrin gel results. (See [5] for a review of fibrinogen, fibrin, and fibrin polymerization.)

The branching process is not well understood. Some important biological polymers have specific molecules that mediate formation of branches. For example, during actin filament formation from actin monomers, the molecule Arp-23 nucleates the formation of new branches [6]. For fibrin, there is no similar molecule, and fibrin gels can form *in vitro* in solutions of fibrinogen and thrombin alone. In these experiments, high thrombin concentrations result in "fine" clots, with relatively thin fibers, a high volume density of branch points, and small pore size. Using thrombin at low concentrations leads to "coarse" clots: thicker fibers, lower branch point density, and larger pores [7]. Recent experiments in which thrombin is produced by reactions on cellular surfaces show variations in clot structure with distance from the surfaces. Fine gels are seen close to the surfaces and a coarser gel more distally, consistent with the expected drop in thrombin concentration with distance from the cells on which it is made [1,8,9]. Studies [10,11] of fibrin polymerization suggest that much of the final gel architecture (branch point density and pore size) is largely determined by the time of gelation, and that most fiber thickening occurs later.

In this paper, we propose a possible mechanism for branch formation during protofibril development, before fibers of appreciable thickness are present. The equations we present for studying this mechanism are a generalization of the equations in the kinetic gelation models studied by Ziff and co-workers [12,13]. The Ziff models track the concentrations c_k of k-mers made from k identical monomers each with n functional units or binding sites. Reactions between functional sites on different molecules lead to the formation of larger polymers and gelation occurs if $n>2$. In our generalization of this type of model, we track concentrations c_{mb} of clusters with b branches and made up from a total of $2m+b$ monomers. We allow two types of reactions which are idealizations of reactions that may occur as protofibrils form. The model takes the form of a (doubly)infinite set of ordinary differential equations. Following the strategy used by Ziff and co-workers, we introduce a moment-generating function, derive a single partial differential equation for this function, and from this PDE derive a small closed set of ordinary differential equations from which we can predict the time of gelation and the structure of the gel at gelation time. Our model differs significantly from prior kinetic modeling

*Corresponding author; fogelson@math.utah.edu
†keener@math.utah.edu

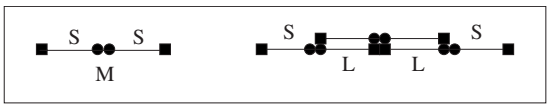

FIG. 1. A monomer M consists of two reacting ends, denoted S. A linear chain consists of any number of links (L) and has two ends S.

of fibrin formation [14–16] because those works did not account for branch formation.

II. FIBRIN CLOT FORMATION MODEL

We regard a fibrin monomer as a long linear molecule comprised of two half-monomer domains denoted S (see Fig. 1). The monomer M has two kinds of binding sites, those at its ends (depicted by a square) and those in the middle (depicted by a circle). A circle of one molecule can bind to a square of another molecule to allow for a staggered polymerization. Because of the staggering, a linear polymer always has two free ends, each of which consists of the half-monomer S. We refer to such a free end as an active site (see Fig. 1). We assume that linear polymerization occurs in two steps. The first step is the binding of the square end of one S domain with the circle end of a different S domain to form a molecule we denote by Z in the reaction $S+S \rightarrow Z$. This molecule can then "zipper" closed to form a completed link $Z \rightarrow L$. In what follows we assume that the initial binding step takes place at a rate $k_s[S]^2$, where by $[S]$ we mean the concentration of free S domains (i.e., active sites), and that the zippering takes place at rate k_z. Thus the formation of a link takes place at a combined rate $k_l[S]^2$, where $k_l=k_z k_s$ (see Fig. 2).

Because the link formation is a two step process, the possibility exists that the zippering step is prevented by binding with other free ends, creating a structure we refer to as a branch (see Fig. 3), in the reaction $Z+S \rightarrow B$. Other higher order polygonal branching structures could also form (see Fig. 13), but including these leads to greater complication without commensurately greater insight. The rate of branch formation from a Z molecule is taken to be $k_B[S]$ so that the combined rate of branch formation is $k_b[S]^3$, where $k_b=k_B k_s$.

In the following, we consider only the two overall reactions, two S domains coming together at rate $k_l[S]^2$ to extend a linear chain, and three S domains coming together at rate $k_b[S]^3$ to form a branch.

With the formation of links and branches as the only two possible reactions, we now examine the formation of clusters. We assume that a cluster can be described by two indices, m and b, where b is the number of branch points, and

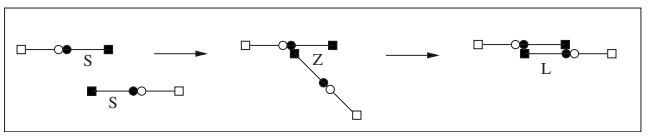

FIG. 2. Half-formed links Z can "zipper" to form a link.

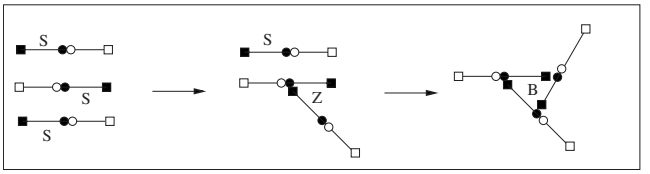

FIG. 3. Half-formed links Z can bind with an end S to form a branch B.

$m+2b$ is the total number of monomers in the cluster. With this notation, a single monomer has $m=1$, $b=0$, and a simple branch (shown in Fig. 3) has $m=1$, $b=1$.

There are two reactions that we allow. The first is the combination of two clusters via linear linking of active sites

$$c_{m_1 b_1} + c_{m_2 b_2} \rightarrow c_{m_1+m_2, b_1+b_2}, \tag{1}$$

and the second is the formation of branch points, assumed to be a trimolecular reaction combining three active sites

$$c_{m_1 b_1} + c_{m_2 b_2} + c_{m_3 b_3} \rightarrow c_{m_1+m_2+m_3-2, b_1+b_2+b_3+1}. \tag{2}$$

We also assume that there are no self interactions between the active sites in a single cluster so that the number of active sites (free ends) in a cluster is $b+2$.

There are several quantities of interest;

$$M = \sum_{m,b} (m+2b) c_{mb} \tag{3}$$

is the total concentration of monomer and

$$A = \frac{1}{M} \sum_{m,b} (m+2b)^2 c_{mb} \tag{4}$$

represents the average cluster size by which we mean the average number of monomers in a cluster. The total concentration of monomer contained in oligomer is $O=M-c_{10}$ and the total concentration of branches is

$$B = \sum_{m,b} b c_{mb}. \tag{5}$$

We define the clot structure parameter p_s as the ratio of the concentration of oligomerized monomer to twice the concentration of branches

$$p_s = \frac{O}{2B}. \tag{6}$$

Gelation is defined to occur when $A \rightarrow \infty$ and the gel time t_g is the time at which this happens. The goal of the following analysis is to determine the structure of the clot at gel time.

To begin this analysis we write the equations governing the dynamics of the cluster-size concentrations c_{mb},

$$\frac{dc_{mb}}{dt} = \frac{k_l}{2}\sum_{b_1+b_2=b}\sum_{m_1+m_2=m}(b_1+2)(b_2+2)c_{m_1b_1}c_{m_2b_2} - k_l(b+2)c_{mb}\sum_{b_1}\sum_{m_1}(b_1+2)c_{m_1b_1} + \frac{k_b}{6} \times \sum_{b_1+b_2+b_3=b-1}\sum_{m_1+m_2+m_3=m+2}(b_1+2)(b_2+2)(b_3+2) \times c_{m_1b_1}c_{m_2b_2}c_{m_3b_3} - \frac{k_b}{2}(b+2)c_{mb} \times \sum_{b_1,b_2}\sum_{m_1,m_2}(b_1+2)(b_2+2)c_{m_1b_1}c_{m_2b_2} + S_{mb}. \quad (7)$$

The first two terms on the right-hand side of Eq. (7) describe the biomolecular reactions and use reaction rates that are the same as used by Ziff and Stell [13]. The next two terms describe the trimolecular reactions and the trimolecular rates use the same fundamental principle. We note that these rates follow the law of mass action when reacting clusters are all different, but deviate from the law of mass action when some of the reacting clusters are the same. The final term S_{mb} in the equation represents the source of clusters of type m,b. Below we make the assumption that only S_{10} is nonzero.

To understand the behavior of this system of equations, we use a generalization of the method used by Ziff and Stell [13]. We introduce the moment generating function,

$$g(y,z) = \sum_{m,b} y^m z^{b+2} c_{mb}, \quad (8)$$

and find that

$$\frac{\partial g}{\partial t} = \frac{k_l}{2}\left(\frac{\partial g}{\partial z}\right)^2 - k_l z\frac{\partial g}{\partial z}R + \frac{k_b}{6y^2}\left(\frac{\partial g}{\partial z}\right)^3 - \frac{k_b}{2}z\frac{\partial g}{\partial z}R^2 + P(y,z), \quad (9)$$

where $R=\Sigma_{m,b}(b+2)c_{mb}$, and $P(y,z)=\Sigma_{m,b}y^m z^{b+2}S_{mb}$. Since S_{10} is the only nonzero source term, $P(y,z)=yz^2S_{10}$.

Next, we need certain moments. To this end, we define quantities

$$M_{jk} = \left.\frac{\partial^{j+k} g}{\partial y^j\, \partial z^k}\right|_{y=1,z=1} \quad \text{and} \quad P_{jk} = \left.\frac{\partial^{j+k} P}{\partial y^j\, \partial z^k}\right|_{y=1,z=1} \quad (10)$$

and note that $R=M_{01}$. We can readily find differential equations for the quantities M_{jk} as follows: first, set $y=z=1$ in Eq. (9) to find

$$\frac{dM_{00}}{dt} = -\frac{k_l}{2}R^2 - \frac{k_b}{3}R^3 + S_{10}. \quad (11)$$

Next, differentiate Eq. (9) with respect to z and set $y=z=1$ to find

$$\frac{dR}{dt} = -k_l R^2 - \frac{k_b}{2}R^3 + 2S_{10}, \quad (12)$$

and then differentiate Eq. (9) again with respect to z, set $y=z=1$ to find

$$\frac{dM_{02}}{dt} = k_l(M_{02}^2 - 2M_{02}R) + k_b(M_{02}^2R - M_{02}R^2) + 2S_{10}. \quad (13)$$

Next, differentiate Eq. (9) with respect to y and set $y=z=1$ to find

$$\frac{dM_{10}}{dt} = -\frac{k_b}{3}R^3 + S_{10}. \quad (14)$$

Taking another derivative with respect to z and setting $y=z=1$ yields

$$\frac{dM_{11}}{dt} = k_l(M_{02}-R)M_{11} + k_bR\left(M_{02}M_{11} - RM_{02} - \frac{1}{2}RM_{11}\right) + 2S_{10}, \quad (15)$$

while taking a second derivative with respect to y and setting $y=z=1$ yields

$$\frac{dM_{20}}{dt} = k_l M_{11}^2 + k_b(RM_{11}^2 + R^3 - 2R^2M_{11}).$$

Now observe that

$$M = M_{01} + 2M_{10} - 4M_{00}$$

and

$$A = \frac{M_{20} + 2M_{11} + M_{02} - 3M_{10} - 3M_{01} - 4M_{00}}{M}.$$

It follows that

$$\frac{dM}{dt} = S_{10},$$

as expected.

Recall that the gel time t_g is defined as the time that A becomes infinite. It follows from Eqs. (11), (12), and (14) that M_{00}, R and M_{10} are bounded functions of time. If M_{02} is bounded, then M_{11} is also bounded since Eq. (15) is linear in M_{11} and hence M_{11} can grow no faster than an exponential. If M_{11} is bounded, then so also is M_{20}. Thus, the gel time is the same as the time when M_{02} becomes unbounded.

Now, define $Y=M_{02}-R$ and find that

$$\frac{dY}{dt} = k_l Y^2 + k_bR\left(\frac{R^2}{2} + RY + Y^2\right), \quad (16)$$

which is a Ricatti equation for Y. We convert this into a linear equation by setting $Y=\frac{U'}{aU}$ and find

$$\frac{d^2U}{dt^2} = -\frac{k_b}{2}aR^3U + \left(k_bR^2 + \frac{a'}{a}\right)\frac{dU}{dt}, \quad (17)$$

where $a=k_l+k_bR$. Note that the variable $U\to 0$ whenever $Y\to\infty$, so $U\to 0$ is an alternative, and more convenient, indication that gelation has occurred. The system of Eqs. (12) and (17) is a closed system which we can solve to determine the gel time.

Other quantities of interest include the free monomer concentration c_{10}, determined by

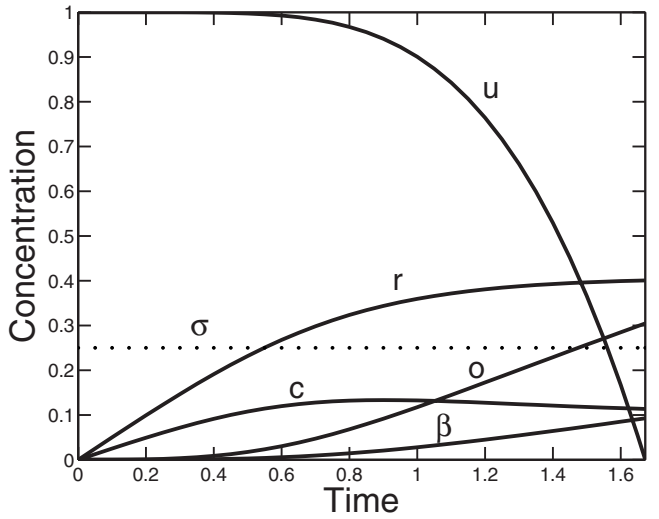

FIG. 4. Behavior in time of the nondimensional variables u, r, β, c, and o for a constant supply rate $\sigma=0.25$ and branching rate $\kappa=10$.

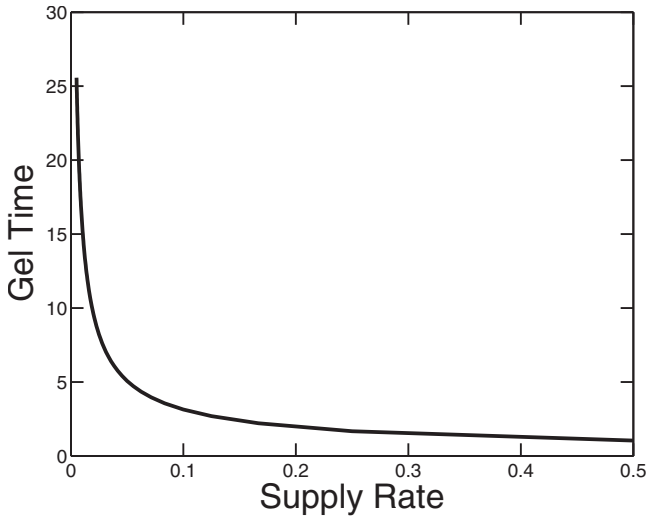

FIG. 5. Nondimensional gel time τ_g as a function of nondimensional supply rate σ. $\kappa=10$.

$$\frac{dc_{10}}{dt} = -(2k_l R + k_b R^2)c_{10} + S_{10}, \tag{18}$$

the total concentration of branches, given by $B=R-2M_{00}$, determined by

$$\frac{dB}{dt} = \frac{k_b}{6}R^3, \tag{19}$$

and the total concentration of monomer contained in oligomer O, determined by

$$\frac{dO}{dt} = S_{10} - \frac{dc_{10}}{dt}. \tag{20}$$

We nondimensionalize the model equations by scaling all concentrations by a typical concentration C_0, scaling time by $(C_0 k_l)^{-1}$, and defining the nondimensional supply rate $\sigma = \frac{S_{10}}{k_l C_0^2}$ and branching rate $\kappa = \frac{k_b C_0}{k_l}$. These are the only two dimensionless parameters in the model. Denoting the dimensionless time by τ, and the nondimensional versions of U, R, B, O, c_{10}, and a by u, r, β, o, c, and α, respectively, the nondimensional equations we study are

$$\frac{d^2u}{d\tau^2} = -\frac{\kappa}{2}\alpha r^3 u + \left(\kappa r^2 + \frac{\alpha'}{\alpha}\right)\frac{du}{d\tau}, \tag{21}$$

$$\frac{dr}{d\tau} = -r^2 - \frac{\kappa}{2}r^3 + 2\sigma, \tag{22}$$

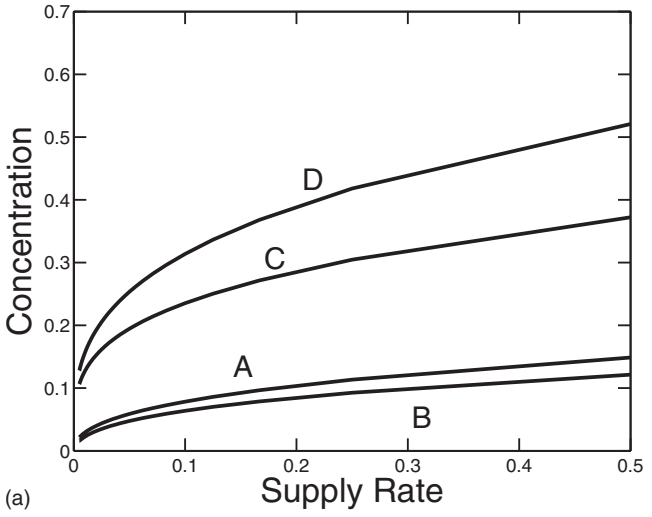

(a)

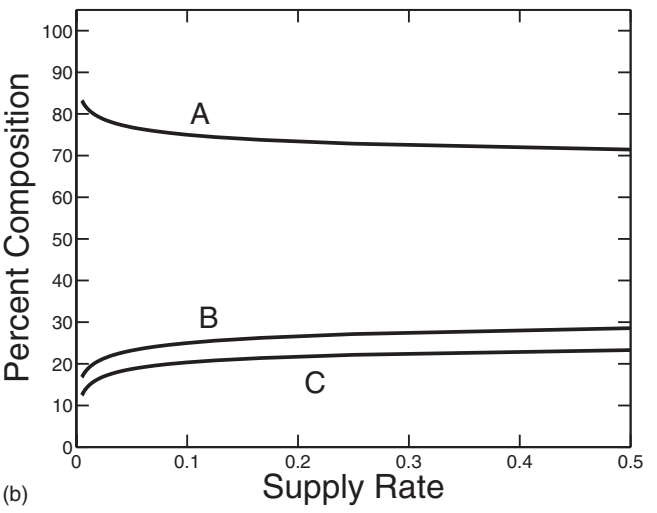

(b)

FIG. 6. (a) Nondimensional concentrations of (A) free monomer, (B) branches, (C) monomer in oligomers, and (D) total monomer at the gel time τ_g as a function of the supply rate σ. (b) Percent composition of fibrin clot at gel time as a function of σ: (A) oligomer, (B) free monomer, and (C) branches. $\kappa=10$.

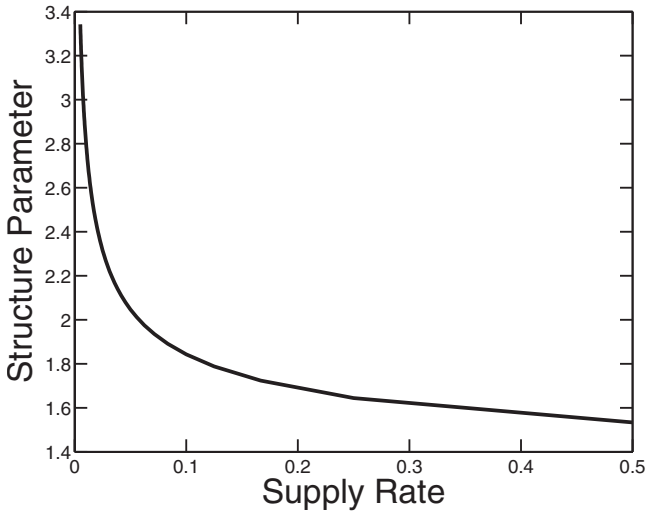

FIG. 7. The structure parameter $o/(2\beta)$ gives an estimate of the mean number of monomers between branch points. It is plotted as a function of nondimensional supply rate σ. $\kappa=10$.

$$\frac{d\beta}{d\tau} = \frac{\kappa}{6} r^3, \tag{23}$$

$$\frac{do}{d\tau} = \sigma - \frac{dc}{d\tau}, \tag{24}$$

$$\frac{dc}{d\tau} = -(2r + \kappa r^2)c + \sigma. \tag{25}$$

where $\alpha = 1 + \kappa r$.

III. RESULTS

We first consider the behavior of the system when monomers are supplied at a constant rate σ. For any constant positive supply rate, the variable u goes to zero at a finite time τ_g and we explore how this gel time and the structure of the gel at that time depend on the monomer supply rate. To find the gel time, we solve Eqs. (21) and (22) with initial conditions $r(0)=0$, $u(0)=1$, and $u'(0)=0$ and find the time τ_g for which $u(\tau_g)=0$. Each simulation is run only up to time τ_g.

Figure 4 illustrates the temporal behavior of the system for a supply rate of $\sigma=0.25$ and a branching rate of $\kappa=10$. The reactive-site concentration r increases monotonically more slowly as the gel time is approached. The free monomer concentration c reaches a maximum at about the time that o and β begin to grow more rapidly, and the gelation indicator function u changes little up to this time and then rapidly drops to zero.

A plot of gel time as a function of the supply rate is shown in Fig. 5. It is no surprise that the gel time is a monotone decreasing function of supply rate. Figure 6 shows various measures of the composition of clusters at the gel time, including the total concentration of oligomer (i.e., the total concentration of monomers that are part of oligomers), the total concentration of free monomer and the total concentration of branches. All of these quantities are increasing functions of supply rate. In the same figure, we see how the relative composition of the clot changes with supply rate. The fraction of monomers incorporated in clusters by gel time decreases, and the ratio of the branch concentration to the total concentration of monomers in oligomers at that time increases as the monomer supply rate grows. This behavior is seen explicitly in Fig. 7, which shows how the structure parameter $p_s=o/(2\beta)$ varies as a function of supply rate. This parameter gives a measure of the average number of monomer units between branch points in an oligomer.

In Fig. 8, we show on a log-log scale how the gel time and structure parameter depend on supply rate for a range of values of the branching rate κ. We see that for each value of κ the plot of gel time against supply rate on a log-log plot decreases linearly with a slope close to $-2/3$. For a fixed supply rate σ, the gel time decreases as the branching rate κ

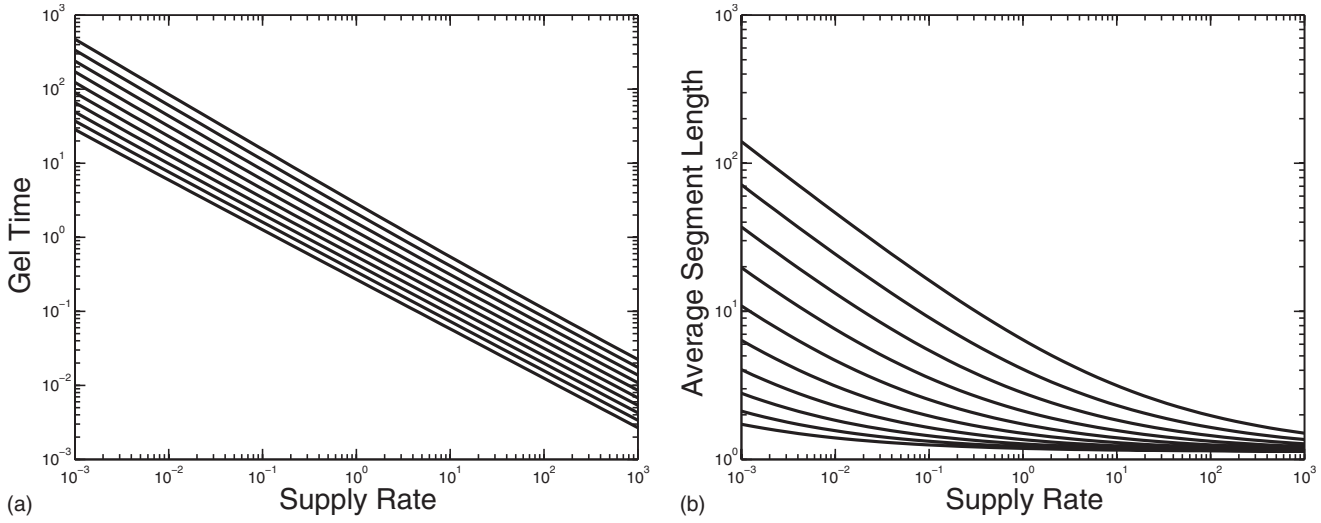

FIG. 8. Variation in gel time τ_g and estimated mean segment length $p_s=o/(2\beta)$ with branching rate κ and monomer supply rate σ. (a) Gel time as a function of σ on a log-log scale, showing power-law behavior. (b) Structure parameter p_s as a function of supply rate. From top to bottom, curves are for branching rates $\kappa=0.25$, 0.50, 1.0, 2.0, 4.0, 8.0, 16.0, 32.0, 64.0, and 128.0.

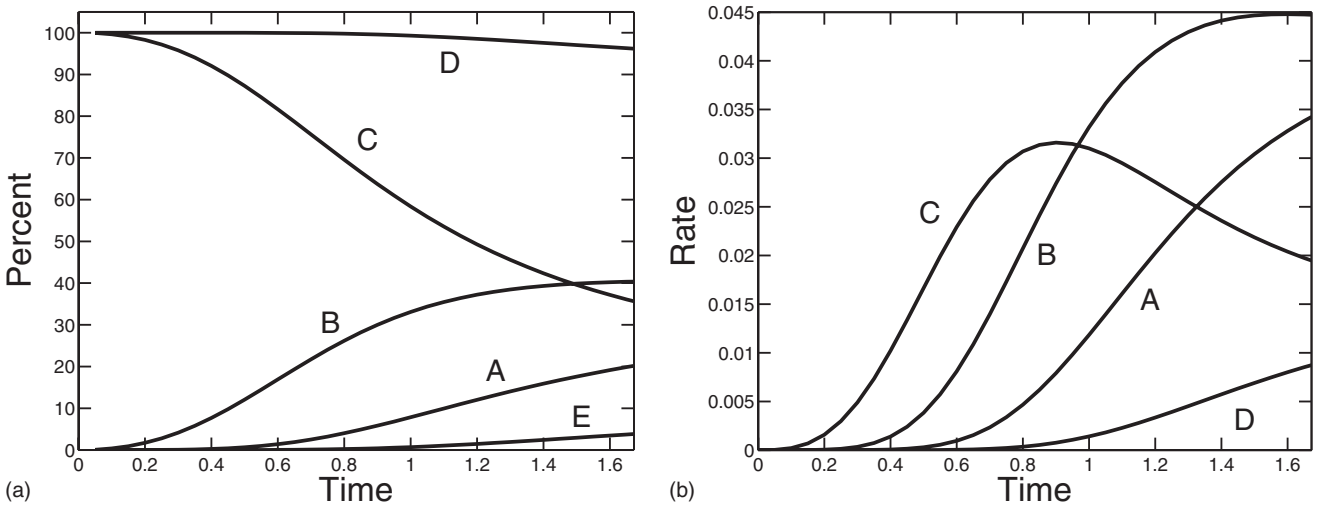

FIG. 9. Formation of branches by different reactions as a function of nondimensional time for monomer supply rate $\sigma=0.25$ and branching rate $\kappa=10$. (a) Curves show percent of branches formed in reactions involving (A) one, (B) two, or (C) three free monomers, the total percent of branches formed in reactions involving at least one free monomer (D), and the percent of branches formed by reactions involving only oligomers (E). (b) Rate of branch formation by reactions that involve (A) one, (B) two, or (C) three monomers, or that involve oligomers only (D).

increases. Log-log plots (not shown) of gel time as a function of the branching rate κ show linear behavior with a slope of approximately $-1/3$. The origin of the two scaling behaviors follows from an approximate analysis of Eqs. (21) and (22). For large κ and moderate σ, Eq. (22) implies that r rapidly equilibrates to the value $r_{ss}=(4\sigma/\kappa)^{1/3}$. Using this value of r in Eq. (21) with $\alpha'=0$ (since r is taken to be constant) and solving for u yields $u=\exp(\kappa r_{ss}^2\tau/2)\cos(\kappa r_{ss}^2\tau/4+\pi/4)$. Using this approximation, we have an estimate of the gel time $\tau_g=\pi/(\kappa r_{ss}^2)=[\pi/(4)^{2/3}]\kappa^{-1/3}\sigma^{-2/3}$.

From the second panel of Fig. 8, we also see that the structure parameter $p_s=o/(2\beta)$ is a decreasing function of supply rate for each fixed value of κ considered. The sensitivity of p_s to supply rate is greater the smaller the branching rate, and, for a given branching rate, the sensitivity is greater at relatively low supply rates.

To understand why the distance between branch points (as estimated by p_s) is a decreasing function of monomer supply rate, we look at the percentage of branches that are formed in reactions that involve one or more monomers and the percentage of branches that are formed with oligomers only. The three ways that branches can form using monomers are with three monomers, two monomers and an oligomer, and one monomer and two oligomers and these are all included in the expression,

$$\kappa c r^2 = \kappa c(r-2c)^2 + 4\kappa c^2(r-2c) + 4\kappa c^3. \tag{26}$$

Here, the first term represents branching with a single monomer and so uses one monomer per branch formed, the second term uses two monomers per branch formed, and the third term uses three monomers per branch formed. It follows that the rate at which *branches* are formed by these reactions is

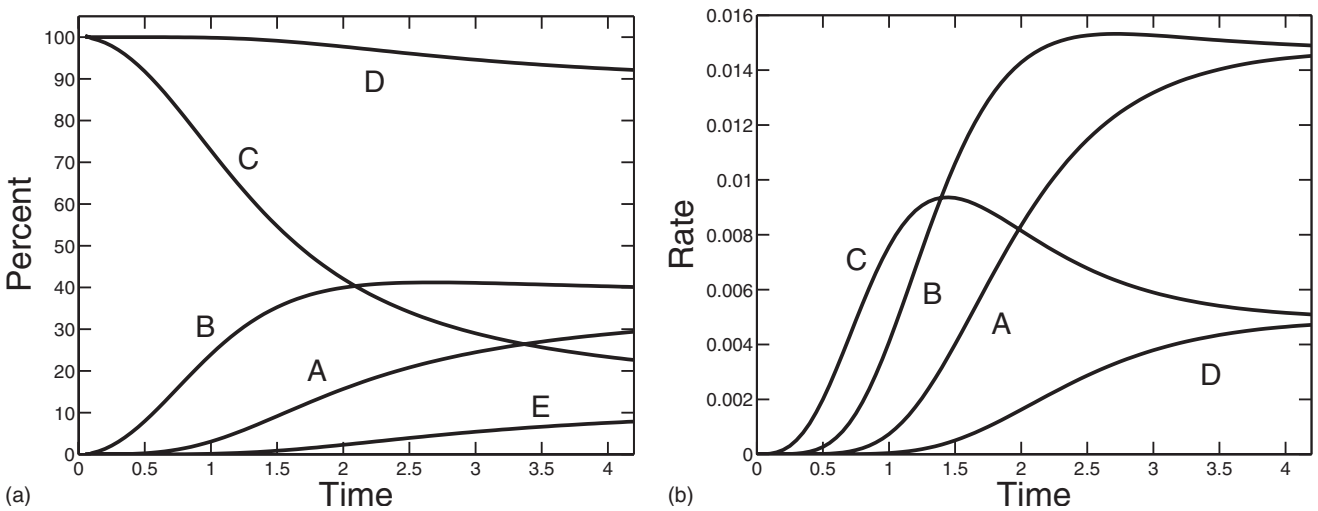

FIG. 10. As in Fig. 9 with $\sigma=0.25$ and $\kappa=1.0$.

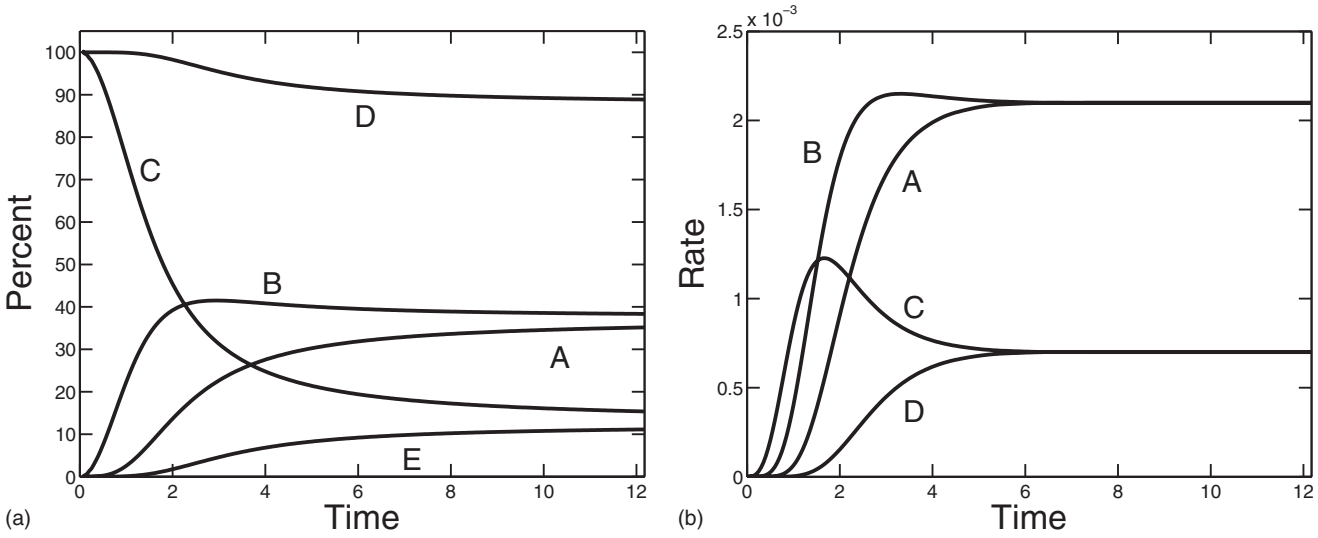

FIG. 11. As in Fig. 9 with $\sigma=0.25$ and $\kappa=0.1$.

$$\kappa c(r-2c)^2 + 2\kappa c^2(r-2c) + \frac{4}{3}\kappa c^3. \tag{27}$$

We integrate each of these three rates to get the total concentrations of branches formed by each of these processes. Our numerical simulations indicate that most of the branches are formed by these three reactions involving monomers rather than by trimerization of three oligomers. This explains why the supply rate of monomers is the major factor in determining the branching structure.

In Figs. 9–11, we show, for a supply rate $\sigma=0.25$, the percent and rate of branches formed by the three types of reaction involving at least one monomer and by the reactions involving oligomers only. The rates for reactions which involve monomers are found from the three rate terms in Eq. (27) and the rate for the reactions using oligomers only is computed by subtracting these three rates from the total rate of branch formation given in Eq. (23). We see that for each of the three branching rates considered $\kappa=10,1,0.1$, the vast majority of branches were formed in reactions that involved at least one monomer. Over a hundredfold variation in the branching constant κ, the percent of branches formed by oligomers alone increased from about 4% to about 11%. For each κ, branch formation from three free monomers dominated early in the polymerization process, but this rate was surpassed first by branch formation reactions that involve two free monomers and one oligomer, and later by reactions that involve one free monomer and two oligomers. If the branch formation rate κ is sufficiently small, the rates at which branches are formed with one monomer or two monomers converge to the same value, as do the rates at which branches are formed with three or zero monomers. This is a consequence of the fact that for low values of κ, the system of Eqs. (21)–(25) can come close to steady state by the time the gel forms, and that the steady state values of r and c are related by $r=4c$.

Figure 12 shows how the time course of polymerization

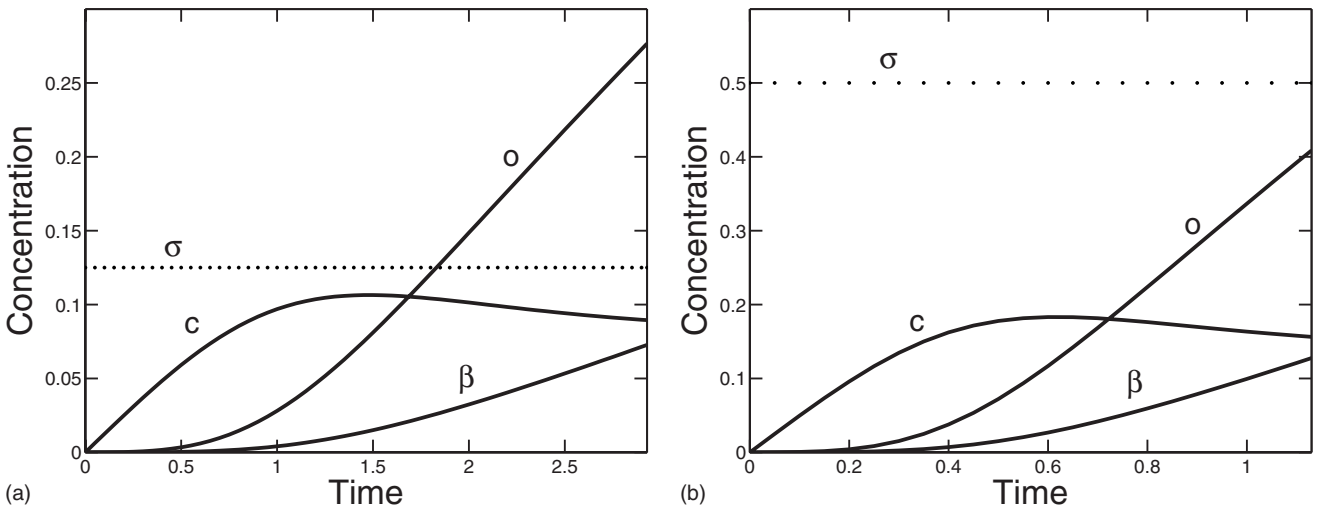

FIG. 12. Behavior in time of the nondimensional variables, β, c, and o for a (a) supply rate $\sigma=0.125$ and branching rate $\kappa=8$, and (b) supply rate $\sigma=0.5$ and branching rate $\kappa=8$.

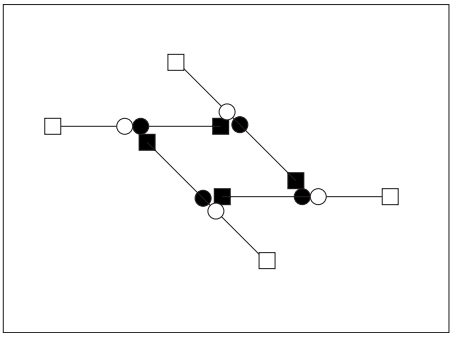

FIG. 13. A branch involving four bonds.

differs for branching rate $\kappa=8$ and two different supply rates $\sigma=0.125$ and $\sigma=0.5$. The extents of oligomer formation and branch formation are both higher at the higher supply rate, but the structure parameter $p_s=o/(2\beta)$ is higher for the lower supply rate (about 3.8 compared to 3).

IV. CONCLUSIONS

We have investigated a mechanism of branch formation during fibrin polymerization. To extend a linear fibrin protofibril, a free end (half-monomer) of another fibrin monomer or cluster must bind to an end of the protofibril. Because this process actually involves two distinct binding steps, a third molecule can interfere with the binding of the original two molecules after the first step but before the second one, and this can lead to formation of a branch. Alternatively the second step may be completed without interference in which case the oligomer grows in size but no branch is formed. Our analysis is based on simplifying this process by combining together the two steps that lead to linear extension into one bimolecular reaction and the two steps that lead to branch formation into a second, trimolecular, reaction. These basic reactions are incorporated into a kinetic gelation model which involves an infinite set of concentrations, one for each population of oligomer consisting of a specific number of branches and made up of a specific number of monomeric units. This model is analyzed, using an approach similar to that of Ziff and co-workers [12,13], for situations in which no monomer is present initially and monomer is supplied at a constant rate up to the time of gelation.

We note that other branching structures are possible, e.g., the four-bond branch shown in Fig. 13. Some form of branch is created whenever an end-to-middle bond forms that interferes with the closing of a Z into a link L. We do not assume that the final form of the branch is determined instantly; that is, there can be a delay between the formation of the two bonds that lead from the situation in the middle picture of Fig. 3 to that in the right picture of that figure. During the delay, other more complicated branching structures can be initiated if a free end of yet another oligomer interferes with the formation of the three-bond branch. The rate of formation of branches with n bonds is proportional to $[S]^n$. The result that branch formation is dependent on monomer supply rate is captured in our model in which only three-bond branches are considered. Inclusion of higher order branching would only reinforce this behavior.

Analysis of our model shows that the time to gelation and the structure of the gel (e.g., mean distance between branch points) at that time depends on the supply rate of monomer. Each monomer is a molecule with two functional active sites, and groups of bifunctional molecules cannot produce a gel. Hence the occurrence of gelation depends on the formation of (trifunctional) branches and the rate and extent of branch formation are increasing functions of the monomer supply rate. The sensitivity of the gel structure to the monomer supply rate varies with the supply rate σ and with the branching rate, which is the rate constant κ for trimolecular reactions. For large values of σ and κ, the structure varies little with changes in the supply rate provided it remains large. For a range of lower values of the supply rate and branching rate, the structure of the gel depends strongly on each of these parameters. Variations in the monomer supply rate are of more physiological interest, and we see that for sufficiently small values of the branching rate, the gel structure parameter p_s changes markedly with changes in σ. For example, we see in Fig. 8 that for $\kappa=1$, changing σ from 1.0 to 0.1 to 0.01 changes p_s from about 3 to about 5.5 to about 15. Thus, the branching mechanism we propose can produce substantially different gel structures for different monomer supply rates consistent with experimental observations [7,10].

The reason that the monomer supply rate can have a strong effect on gel structure is that most branches are formed in reactions that involve at least one monomer. Early in the polymerization process, three monomer reactions dominate; later one monomer and two monomer ones occur more rapidly. Thus the availability of monomers is critical to the rate at which branches form throughout the gelation process.

We have not yet attempted to combine this model with a model that predicts the time variation of thrombin formation [17–19] and the rate of conversion of fibrinogen to fibrin monomer by thrombin. It will be interesting to see the fibrin structures that result when we do so, and further to see how spatial heterogeneities in thrombin concentration when it forms under flow and in the presence of platelets translates into spatial patterns in the gel structure. We note also that there is a mode of branch point formation that is different from that considered here, namely, divergence of two protofibrils during lateral assembly. Determining whether this alternative mode of branching would result in the gel structure being sensitive to monomer supply rate will be the subject of future modeling work.

ACKNOWLEDGMENTS

The authors thank John Weisel and Bob Guy for many helpful discussions. This work was supported, in part, by NSF Grant No. DMS-0540779 and by NIGMS Grant No. R01-GM090203.

[1] J. Weisel, J. Thromb. Haemostasis **5**, 116 (2007).
[2] J. P. Collet, D. Park, C. Lesty, J. Soria, C. Soria, G. Montalescot, and J. W. Weisel, Arterioscler., Thromb., Vasc. Biol. **20**, 1354 (2000).
[3] K. Fatah, A. Silveria, P. Tornvall, F. Karpe, M. Blomback, and A. Hamsten, Thromb. Haemostasis **76**, 535 (1996).
[4] A. S. Wolberg and R. A. Campbell, Transfus. Apher. Sci. **38**, 15 (2008).
[5] J. W. Weisel, Adv. Protein Chem. **70**, 247 (2005).
[6] T. Pollard, Annu. Rev. Biophys. Biomol. Struct. **36**, 451 (2007).
[7] E. A. Ryan, L. F. Mockros, J. W. Weisel, and L. Lorand, Biophys. J. **77**, 2813 (1999).
[8] R. A. Campbell, K. A. Obermyer, C. R. Bagnell, and A. S. Wolberg, Arterioscler., Thromb., Vasc. Biol. **28**, 2247 (2008).
[9] R. A. Campbell, K. A. Obermyer, C. H. Selzman, B. C. Sheridan, and A. Wolberg, Blood **114**, 4886 (2009).
[10] B. Blombäck, K. Carlsson, K. Fatah, B. Hessel, and R. Procyk, Thromb. Res. **75**, 521 (1994).
[11] I. Chernysh and J. Weisel, Blood **111**, 4854 (2008).
[12] R. M. Ziff, J. Stat. Phys. **23**, 241 (1980).
[13] R. M. Ziff and G. Stell, J. Chem. Phys. **73**, 3492 (1980).
[14] R. D. Guy, A. L. Fogelson, and J. P. Keener, IMA J. Math. Appl. Med. Biol. **24**, 111 (2007).
[15] R. R. Hantgan and J. Hermans, J. Biol. Chem. **254**, 11272 (1979).
[16] J. W. Weisel and C. Nagaswami, Biophys. J. **63**, 111 (1992).
[17] A. L. Fogelson and N. Tania, Pathophysiol. Haemost. Thromb. **34**, 91 (2005).
[18] K. Leiderman and A. L. Fogelson, IMA J. Math. Appl. Med. Biol. **34**, 91 (2005).
[19] A. L. Kuharsky and A. L. Fogelson, Biophys. J. **80**, 1050 (2001).